"Nanoscale Zippers" in the Crystalline Solid. Structural Variations in the Giant Magnetocaloric Material $Gd_5Si_{1.5}Ge_{2.5}$

Wonyoung Choe,[†,§] Gordon J. Miller,*[,†] John Meyers,[‡] Scott Chumbley,[‡] and A. O. Pecharsky[‡]

Department of Chemistry and Department of Materials Science and Engineering, Ames Laboratory, U.S. Department of Energy, Iowa State University, Ames, Iowa 50011

Received September 9, 2002. Revised Manuscript Received January 7, 2003

The magnetocaloric material $Gd_5Si_{1.5}Ge_{2.5}$ has been synthesized and its crystal structures at 292 and 163 K are reported from single-crystal X-ray diffraction experiments. At room temperature, orthorhombic Sm_5Ge_4-type and twinned, monoclinic $Gd_5Si_2Ge_2$-type phases coexist in single crystal specimens. This phenomenon is mainly due to the covalent bond breaking and formation of (Si,Ge)−(Si,Ge) dimers during the crystallographic phase transition. We suggest an atomic-level model for the interface of the two distinct domains. A detailed TEM analysis also confirms the coexistence of both phases in a polycrystalline sample. The structural relationship between such nanoscale zippers and other known phases is identified.

Introduction

The unprecedented giant magnetocaloric effect (MCE)[1] found in $Gd_5(Si_xGe_{1-x})_4$, along with other unique magnetic properties such as a colossal magnetostriction[2] and giant magnetoresistance,[3] has initiated vigorous research activities on this and related lanthanide systems.[4] Further studies show that the giant MCE found in $Gd_5Si_2Ge_2$ is due to a first-order phase transformation on heating, when a ferromagnetic to paramagnetic transition at ca. 277 K is coupled with the orthorhombic Gd_5Si_4-type to monoclinic $Gd_5Si_2Ge_2$-type crystallographic transition.[5] Temperature-dependent, single-crystal X-ray studies of $Gd_5Si_2Ge_2$ show that the magnetic transition accompanies a simultaneous structural transition, which involves reversible covalent bond cleavage and formation while maintaining its crystallinity throughout the transition.[6] Such a single crystal to single crystal phase transformation with covalent bond-breaking and reforming is an extremely rare phenomenon,[7] although examples involving weaker interatomic interactions such as van der Waals forces and hydrogen bonding are more frequently found.[8]

The structural phase transitions in $Gd_5(Si_xGe_{1-x})_4$ can be induced by changing temperature, magnetic field, pressure, and/or the Si/Ge ratio.[5] As the Si content increases, the room-temperature crystal structures of $Gd_5(Si_xGe_{1-x})_4$ vary from the orthorhombic Sm_5Ge_4-type ($0 < x \leq 0.3$) to the monoclinic $Gd_5Si_2Ge_2$-type ($0.400 < x \leq 0.503$), and further to the Gd_5Si_4-type ($0.575 \leq x \leq 1$) in a paramagnetic state, while in a ferromagnetic state the crystal structures are all Gd_5Si_4-type, regardless of x.[9,10] These three structure types[11] can be constructed from $^{\infty}_{2}[Gd_5(Si_xGe_{1-x})_4]$ slabs held together by (Si,Ge) atoms.[12] One of the most drastic differences that exists between these types is the interslab bonds

* To whom correspondence should be addressed. E-mail: gmiller@iastate.edu.

† Department of Chemistry.

‡ Department of Materials Science and Engineering.

§ Present address: CMS Division, Lawrence Livermore National Laboratory, Livermore, CA.

(1) (a) Pecharsky, V. K.; Gschneidner, K. A., Jr. *Phys. Rev. Lett.* **1997**, *78*, 4494−4497. (b) Pecharsky, V. K.; Gschneidner, K. A., Jr. *Appl. Phys. Lett.* **1997**, *70*, 3299. (c) Pecharsky, V. K.; Gschneidner, K. A., Jr. *J. Magn. Magn. Mater.* **1997**, *167*, L179−184. (d) Giguere, A.; Foldeaki, M.; Ravi Gopal, R.; Bose, T. K.; Frydman, A. *Phys. Rev. Lett.* **1999**, *83*, 2262. (e) Gschneidner, K., Jr.; Pecharsky, V. K.; Brück, E.; Duijin, H. G. M.; Levin, E. M. A. *Phys. Rev. Lett.* **2000**, *85*, 4190.

(2) (a) Morellon, L.; Blasco, J.; Algarabel, P. A.; Ibara, M. R. *Phys. Rev. B* **2000**, *62*, 1022. (b) Morellon, L.; Algarabel, P. A.; Ibara, M. R.; Blasco, J. *Phys. Rev. B* **1998**, *58*, R14721. (c) Chernyshov, A. S.; Filippov, D. A.; Ilyn, M. I.; Levitin, R. Z.; Pecharskaya, A. O.; Pecharsky, V. K.; Gschneidner, K. A., Jr.; Snegirev, V. V.; Tishin, A. M. *Phys. Met. Metallogr.* **2002**, *93*, S19.

(3) (a) Morellon, L.; Stankiewicz, J.; Gracia-Landa, B.; Algarabel, P. A.; Ibara, M. R. *Appl. Phys. Lett.* **1998**, *73*, 3462. (b) Levin, E. M.; Pecharsky, V. K.; Gschneidner, K. A., Jr. *Phys. Rev. B* **1999**, *60*, 7993. (c) Levin, E. M.; Pecharsky, V. K.; Gschneidner, K. A., Jr. *J. Magn. Magn. Mater.* **2000**, 210, 181.

(4) (a) Spichkin, Y. I.; Pecharsky, V. K.; Gschneidner, K. A., Jr. *J. Appl. Phys.* **2001**, *89*, 1738. (b) Ivtchenko, V. V.; Pecharsky, V. K.; Gschneidner, K. A., Jr. *Adv. Cryog. Eng.* **2000**, *46*, 405. (c) Gschneidner, K. A., Jr.; Pecharsky, V. K.; Pecharsky, A. O.; Ivtchenko, V. V.; Levin, E. M. *J. Alloys Compd.* **2000**, *303−304*, 214. (d) Ritter, C.; Morellon, L.; Algarabel, P. A.; Magen, C.; Ibara, M. R. *Phys. Rev.* **2002**, *65*, 094405. (e) Tegus, O.; Dagula, O.; Bruck, E.; Zhang L.; de Boer, F. R.; Buschow, K. H. J. *J. Appl. Phys.* **2002**, *91*, 8534.

(5) For a review on the $Gd_5(Si_xGe_{1-x})_4$ system, see Pecharsky, V. K.; Gschneidner, K. A., Jr. *Adv. Mater.* **2001**, *13*, 683.

(6) (a) Choe, W.; Pecharsky, V. K.; Pecharsky, A. O.; Gschneidner, K. A., Jr.; Young, V. G., Jr.; Miller, G. J. *Phys. Rev. Lett.* **2000**, *84*, 4617.

(7) One example is the reversible polymerization of fullerene cages. See Stephens, P. W.; Bortel, G. Faigel, G.; Tegze, M.; Janossy, A.; Pekker, S.; Oszlanyi, G.; Forro, L. *Nature* **1994**, *370*, 636.

(8) (a) Reetz, M. T.; Hoeger, S.; Harms, K. *Angew. Chem., Int. Ed. Engl.* **1994**, *33*, 181−183. (b) Dattelbaum, A. M.; Martin, J. D. *Inorg. Chem.* **1999**, *38*, 2369−2374. (c) Libowitzky, E.; Armbruster, T. *Am. Mineral.* **1995**, *80*, 1277−1285. (d) Boese, R.; Miebach, T.; De Meijere, A. *J. Am. Chem. Soc.* **1991**, *113*, 1743. (e) Ye, J.; Soeda, S.; Nakamura, Y.; Nittono, O. *J. Appl. Phys. 1* **1998**, *37*, 4264.

(9) Pecharsky, A. O.; Gschneidner, K. A., Jr.; Pecharsky, V. K.; Schindler, C. E. *J. Alloys Compd.* **2002**, *338*, 126.

10.1021/cm020928l CCC: $25.00
Published on Web 03/04/2003

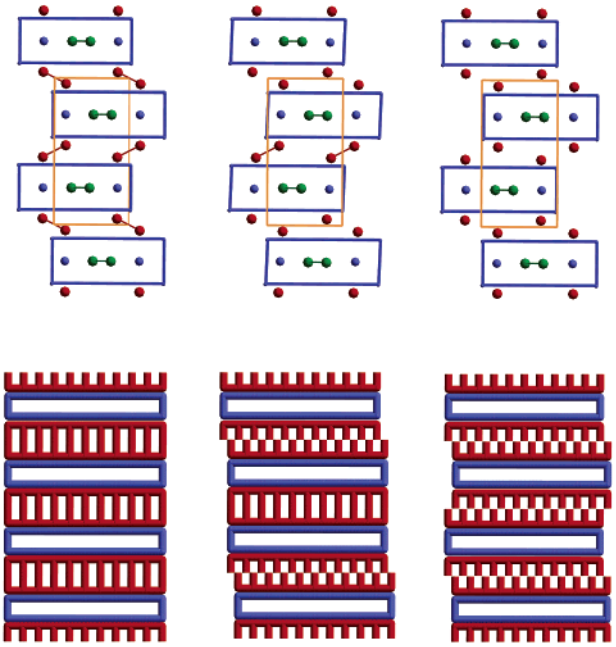

Figure 1. Three structure types found in $Gd_5(Si_xGe_{1-x})_4$. (left) Gd_5Si_4-type; (middle) $Gd_5Si_2Ge_2$-type; (right) Sm_5Ge_4-type. Blue rectangular boxes indicate $^{\infty}_{2}[Gd_5(Si_xGe_{1-x})_4]$slabs. Inside these slabs (Si,Ge)−(Si,Ge) dimers (green), together with Gd atoms (blue) reside. The (Si,Ge) atoms between the slabs are shown in red. Orange lines indicate unit cells. Top: Three structures to highlight the dimer formation/cleavage between the $^{\infty}_{2}[Gd_5(Si_xGe_{1-x})_4]$slabs. Bottom: Three nanoscale zippers in $Gd_5(Si_xGe_{1-x})_4$. The bond cleavage/ formation is shown as shear movement of $^{\infty}_{2}[Gd_5(Si_xGe_{1-x})_4]$slabs. Solid/broken lines between the blue slabs indicate dimer formation/cleavage, respectively.

of the (Si, Ge) atoms. All of the (Si, Ge) atoms between the $^{\infty}_{2}[Gd_5(Si_xGe_{1-x})_4]$ slabs occur in dimers in the Gd_5Si_4-type with an interatomic distance of ca. 2.6 Å. In the $Gd_5Si_2Ge_2$-type, one-half of these dimers break into two "isolated" (Si,Ge) atoms and, finally, in the Sm_5Ge_4-type all of these (Si,Ge) atoms are "isolated."[10d] This action is reminiscent of a "zipper," if we consider the opening and closing action of a zipper as breaking and reforming interslab covalent bonds (Figure 1). Kanatzidis and co-workers discovered a similar "zipping action" in single-crystal to single-crystal successive oxidative transformations from $Cs_3Bi_7Se_{12}$ to $Cs_2Bi_7Se_{12}$, and further to $CsBi_7Se_{12}$.[13] In the $Gd_5(Si_xGe_{1-x})_4$ system we call these "nanoscale zipper" structures, because the zipping action across the [010] direction is within nanometer regime.

An important difference among the three structure types in this series is the average formal charge of Si and Ge. As the structure changes from the Gd_5Si_4-type to the $Gd_5Si_2Ge_2$-type and to the Sm_5Ge_4-type, the respective charge-balanced formulas based on the Zintl−Klemn formalism are $[(Gd^{3+})_5(T_2^{6-})_2(3e^-)]$, $[(Gd^{3+})_5((T_2^{6-})_{1.5}(T^{4-})(2e^-)]$, and $[(Gd^{3+})_5(T_2^{6-})(T^{4-})_2(1e^-)]$, where T represents Si or Ge. Note that the number of electrons assigned to the conduction band drops as some of the T_2 bonds break. Essentially, this remarkable series demonstrates sequential redox reactions taking place in the solid state. Therefore, subtle differences in the Si/Ge ratio, temperature, pressure, or magnetic field can create a "nanoscale zipper" composed of (Si,Ge)−(Si,Ge) dimers across the two-dimensional $^{\infty}_{2}[Gd_5(Si_xGe_{1-x})_4]$ slabs in the Gd_5Si_4−Gd_5Ge_4 isoplethic system (NOTE: Gd_5Ge_4 does not melt congruently, so this system is strictly not "pseudo-binary").

In this paper we examine $Gd_5Si_{1.5}Ge_{2.5}$ from the $Gd_5(Si_xGe_{1-x})_4$ system ($x = 0.375$), which lies between the extended solid solution with the orthorhombic Sm_5Ge_4-type ($0 < x \leq 0.3$) and the monoclinic $Gd_5Si_2Ge_2$-type ($0.4 < x < 0.503$) alloys at room temperature[9] using temperature-dependent, single-crystal X-ray diffraction together with transmission electron microscopy (TEM) and selected area diffraction (SAD). Our motivation for this structural study is 2-fold. One is to find possible relationships between the crystal structure and the magnetic properties reported for the title compound. As prepared, $Gd_5Si_{1.5}Ge_{2.5}$ exists in a two-phase region between two different structure types under ambient conditions,[9] and might exhibit unique physical properties that cannot be seen in either structure type. In fact, the magnetic measurements indicate an intermediate heterogeneous state in the vicinity of the first-order phase transition for this phase.[14a] Furthermore, electrical resistivity measurements on $Gd_5Si_{1.5}Ge_{2.5}$ also show peculiar behavior compared to that of $Gd_5Si_2Ge_2$.[14b] Despite such efforts, the underlying principle behind these observations has not been fully understood. The second purpose of this study is directed toward an exploratory synthetic issue. The monoclinic phase of $Gd_5Si_2Ge_2$ can be considered as a 1:1 intergrowth of Gd_5Si_4 (Gd_5Si_4-type) and Gd_5Ge_4 (Sm_5Ge_4-type),[7] because its crystal structure has an equal portion of both structural motifs. Similarly, $Gd_5Si_{1.5}Ge_{2.5}$ could be another intergrowth compound between Gd_5Ge_4 (Sm_5Ge_4-type) and $Gd_5Si_2Ge_2$ ($Gd_5Si_2Ge_2$-type). For example, a hypothetical intergrowth pattern is a 1:3 combination of Gd_5Ge_4 (Sm_5Ge_4-type) and $Gd_5Si_2Ge_2$ ($Gd_5Si_2Ge_2$-type), i.e., $^1/_4Gd_5Ge_4 + {}^3/_4Gd_5Si_2Ge_2 = Gd_5Si_{1.5}Ge_{2.5}$.

We report here the single crystal as well as detailed surface structures of polycrystalline $Gd_5Si_{1.5}Ge_{2.5}$. We find the coexistence of the monoclinic $Gd_5Si_2Ge_2$-type and the orthorhombic Sm_5Ge_4-type in crystalline samples of $Gd_5Si_{1.5}Ge_{2.5}$. The difference in the nanoscale "zipping action" of (Si,Ge)−(Si,Ge) dimers between the

(10) (a) The two end members of the ternary $Gd_5(Si_xGe_{1-x})_4$ system, Gd_5Ge_4[10b] (Sm_5Ge_4-type) and Gd_5Si_4 (Gd_5Si_4-type),[10c] have been known for over 30 years. For $Gd_5Si_2Ge_2$ type, see ref 6. The main differences between these types are the x/a positional parameters of selected atomic sites.[10d] (b) Holtzberg, F.; Gambino, R. J.; McGuire, T. R. *J. Phys. Chem. Solids* **1967**, *28*, 2283. (c) Smith, G. S.; Johnson, Q.; Tharp, A. G. *Acta Crystallogr.* **1967**, *22*, 269. (d) Cromer, D. T. *Acta Crystallogr.* **1977**, *B33*, 1993.

(11) (a) Pecharsky, V. K.; Gschneidner, K. A., Jr. *J. Alloys Compd.* **1997**, *260*, 98. (b) Liu, Q. L.; Rao, G. H.; Yang, H. F.; Liang, J. K. *J. Alloys Compd.* **2001**, *325*, 50. (c) ref 2. (d) Liu, Q. L.; Rao, G. H.; Liang, J. K. *Rigaku J.* **2001**, 18, 46−50. (e) The two-phase region between the Sm_5Ge_4- and $Gd_5Si_2Ge_2$-type solid solutions for $0.3 < x < 0.4$ in $Gd_5(Si_xGe_{1-x})_4$ has been a controversial region. The authors in ref 11b assigned $Gd_5(Si_{0.3}Ge_{0.7})_4$ as the monoclinic $Gd_5Si_2Ge_2$-type, but the those in ref 9 assigned it as the orthorhombic Sm_5Ge_4-type.

(12) The slabs found in the $Gd_5(Si_xGe_{1-x})_4$ system are identical to ones in the U_3Si_2-type. See Choe, W.; Levin, E. M.; Miller, G. J. *J. Alloys Compd.* **2001**, *329*, 121 and references therein.

(13) For examples of topotactic single-crystal to single-crystal transformations, see Iodanidis, L.; Kanatzidis, M. G. *J. Am. Chem. Soc.* **2000**, *122*, 8319 and references therein.

(14) (a) Levin, E. M.; Gschneidner, K. A., Jr.; Pecharsky, V. K. *J. Magn. Magn. Mater.* **2001**, *231*, 135. (b) Levin, E. M.; Gschneidner, K. A., Jr.; Pecharsky, V. K. Tomlinson, P. *J. Magn. Magn. Mater.* **2000**, *210*, 181.

$^{\infty}_{2}[Gd_5(Si_xGe_{1-x})_4]$ slabs creates structural variation in polycrystalline $Gd_5Si_{1.5}Ge_{2.5}$. An analysis of transmission electron microscopy (TEM) and selected area diffraction (SAD) of polycrystalline $Gd_5Si_{1.5}Ge_{2.5}$ also confirms the coexistence of both phases.

Experimental Section

Synthesis. The purity of Gd is a critical issue because small amounts of impurities can significantly reduce the magnetocaloric effect. We used a high quality Gd metal (99.99 wt. %+) obtained from the Materials Preparation Center of the Ames Laboratory. The major impurities were (in ppm atomic) O, ~300−1000; C,~100−350; N, ~50−300; F, ~25−100; and Fe, ~16−35. Si (99.9999%) and Ge (99.9999%) powders were obtained from CERAC, Inc. The $Gd_5Si_{1.5}Ge_{2.5}$ sample examined in this study was prepared by arc-melting its constituent elements in an argon atmosphere on a water-cooled copper hearth. The resulting button was remelted several times and turned over after each melting to ensure homogeneity. Single crystals were selected from the as-cast sample. Because preliminary thermal analysis studies indicate that $Gd_5Si_{1.5}Ge_{2.5}$ forms peritectically from the melt, this method of obtaining single crystals minimizes the formation of $Gd_5(Si_xGe_{1-x})_3$ and $Gd(Si_xGe_{1-x})$.[9] Analysis of the final product using semiquantitative energy-dispersive spectroscopy (EDS) attached to a scanning electron microscope (SEM) indicated that the average composition is $Gd_5Si_{1.52(3)}Ge_{2.48(3)}$. The room-temperature X-ray powder diffraction pattern for $Gd_5Si_{1.5}Ge_{2.5}$ also shows that the bulk sample is a two-phase alloy with the monoclinic $Gd_5Si_2Ge_2$-type and orthorhombic Sm_5Ge_4-type phases.[9] Annealing the sample for 3 days at 1270 K, which was performed for the samples examined in ref 14a, does not give an X-ray powder diffraction pattern different from that of the as-cast samples, but does create crystals of poorer quality for single-crystal X-ray diffraction experiments. The EDS analysis indicates that the compositional variations across the bulk sample are negligible, suggesting that the compositional difference between the orthorhombic and monoclinic phases is very small.

Transmission Electron Microscopy. The $Gd_5Si_{1.5}Ge_{2.5}$ sample was mechanically thinned to 140 μm, reinforced with epoxy and a single-slit Mo support grid, and then mechanically dimpled until the center of the specimen was perforated. During the dimpling process the sample was reinforced with epoxy again after cracks started to appear. The sample was ion-milled at 4.5 kV, 15 degrees, and 1 mA for 1.5 h to clean the surface. TEM bright field images (BF) and SAD patterns were taken of the sample both off and on zone axes.

Single-Crystal X-ray Crystallography. X-ray diffraction data of single crystals of $Gd_5Si_{1.5}Ge_{2.5}$ were collected using a Bruker CCD-1000 diffractometer, operating at 50 kV/40 mA, with Mo Kα radiation ($\lambda = 0.71073$ Å) and a detector-to-crystal distance of 5.08 cm. Data were collected in at least a quarter hemisphere and were harvested by collecting three sets of frames with 0.3° scans in ω for an exposure time of 10−20 s per frame (for the crystals discussed in subsequent sections, data were collected in a half hemisphere). The range of 2θ extended from 3.0° to 56.0°. The reflections were extracted from the frame data using the SMART program[15] and then integrated using the SAINT program.[15] Data were corrected for Lorentz and polarization effects. Absorption corrections using SADABS[15] were based on fitting a function to the empirical transmission surface as sampled by multiple equivalent reflections. Unit cell parameters were indexed by peaks obtained from 90 frames of reciprocal space images and then refined using all observed diffraction peaks after data integration. The structure solution was obtained by direct methods and refined by full-matrix least-squares refinement of F_o^2 using the Bruker SHELXTL package.[15]

(15) SMART, SAINT, SHELXTL, and SADABS. Bruker Analytical X-ray Instruments Inc.: Madison, WI, 2001.

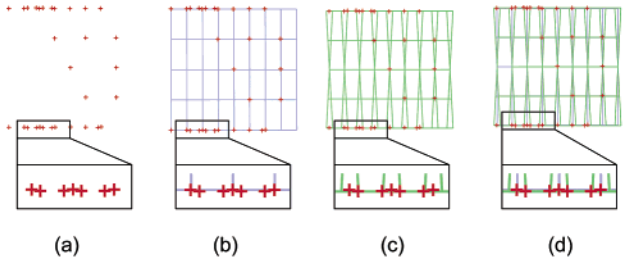

Figure 2. ($hk1$) Reciprocal lattice slice of crystal **1**. (a) ($hk1$) reflections extracted from CCD frame data. The same reflections with (b) orthorhombic Sm_5Ge_4-type grid, (c) twinned, monoclinic $Gd_5Si_2Ge_2$-type grids, (d) orthorhombic and monoclinic grids superimposed simultaneously. In (b) and (c), note that some reflections are incompatible with the grids, whereas in (d) all reflections match with the grids.

Table 1. Crystallographic Data for Crystal 3 of $Gd_5(Si_{1.5}Ge_{2.5})$

temperature	163 K	292 K
space group	*Pnma*	*Pnma*
a, Å	7.517(3)	7.6583(9)
b, Å	14.800(5)	14.7934(18)
c, Å	7.790(3)	7.7554(9)
V, Å^3	866.6(5)	878.63(18)
w*R*2, [$I > 2\sigma(I)$]	0.0944	0.0981
*R*1, [$I > 2\sigma(I)$]	0.0403	0.0392

Results and Discussion

Structure Refinement. The first $Gd_5Si_{1.5}Ge_{2.5}$ crystal selected (hereafter, referred as crystal **1**) has a crystallographic problem when we attempt to solve the data set based on the orthorhombic Sm_5Ge_4-type. Although the cell parameters match well with the ones from the Sm_5Ge_4-structure type ($a = 7.647(1)$ Å, $b = 14.77(2)$ Å, $c = 7.768(2)$ Å), the *R* value is quite high: R = 0.1029 [$I > 2\theta(I)$] for 50 parameters and 848 reflections. Although the bond distances from this initial structural model are all chemically reasonable, significant electron residues are present near every Gd site i.e., the highest one is 23.7 e$^-$/Å^3 located 0.9 Å from Gd1 site (Table 1), indicating that our preliminary structural model is far from the correct one.

Therefore, we carefully examined the reciprocal lattice grids extracted from the CCD frame data. The ($hk1$) reciprocal lattice slice of crystal **1** is shown in Figure 2. Several peculiar features are noticeable. (1) The reflections cannot be indexed to a single set of cell parameters (Figure 2a). (2) If we try to index these reflections with the orthorhombic Sm_5Ge_4-type cell, a significant number of reflections are incompatible (Figure 2b). (3) The same is true for the monoclinic $Gd_5Si_2Ge_2$-type cell (Figure 2c). (4) However, if we superimpose the orthorhombic and monoclinic grids together, as shown in Figure 2d, all observed reflections can be indexed to either the orthorhombic Sm_5Ge_4-type or a twinned, monoclinic $Gd_5Si_2Ge_2$-type cell.[16,17] The orthorhombic and monoclinic cells obtained from the pattern are oriented in such a way that they share the reciprocal axis **b***. The monoclinic cell parameters obtained are $a = 7.624(4)$ Å, $b = 14.848(8)$ Å, $c = 7.809(4)$ Å, and $\beta = 93.08(1)°$, which agree well with the $Gd_5Si_2Ge_2$-type.

Judging from the ($hk1$) lattice slice, crystal **1** contains two different crystalline domains, namely ca. 30% monoclinic $Gd_5Si_2Ge_2$-type and ca. 70% orthorhombic Sm_5Ge_4-type (Figure 3a). The fraction of each phase can be estimated by comparing the three strongest reflections of each phase. It is assumed that the three

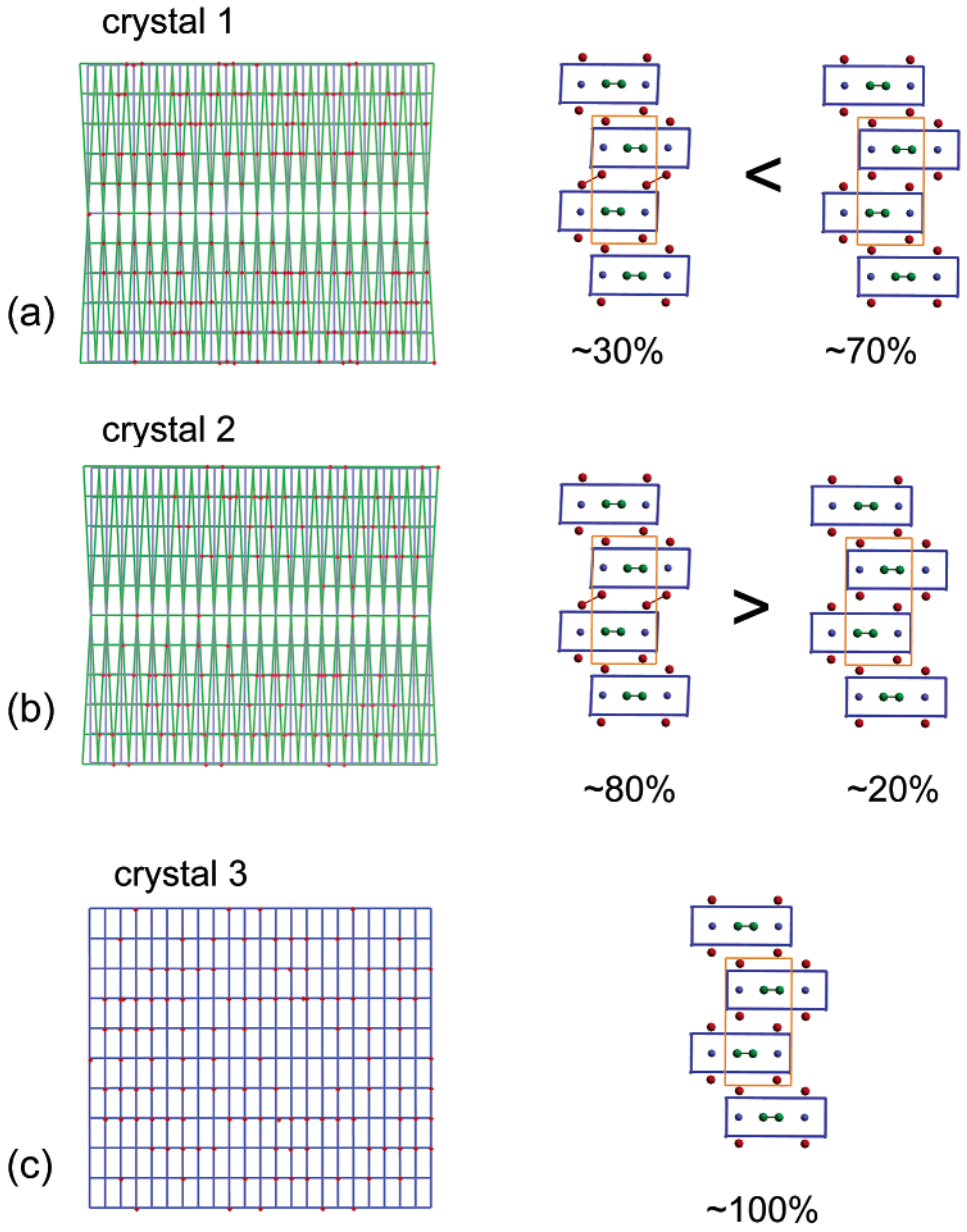

Figure 3. (*hk*1) reciprocal lattice slices of (a) crystal **1**, (b) crystal **2**, and (c) crystal **3**. On the basis of the relative intensities of both monoclinic and orthorhombic phases (see text for details), the proportions between orthorhombic and monoclinic phases are shown.

strongest reflections in the orthorhombic phase are the same as those in the monoclinic phase. Interestingly, the ratio of the two distinct crystalline domains varies among different crystals. For example, a second crystal (crystal **2** hereafter) shows a similar, but different (*hk*1) lattice slice (Figure 3b). The difference is the relative intensities between the two crystalline domains. Crystal **2** has ca. 80% of the monoclinic $Gd_5Si_2Ge_2$-type and ca. 20% of orthorhombic Sm_5Ge_4-type. The cell parameters obtained from crystal **2** are $a = 7.607(4)$ Å, $b = 14.824(8)$ Å, $c = 7.795(4)$ Å, and $\beta = 93.23(1)°$ for the $Gd_5Si_2Ge_2$-type and $a = 7.611(6)$ Å, $b = 14.87(1)$ Å, and $c = 7.798(6)$ Å for the Sm_5Ge_4-type. The refinement based on the major phase in **2**, i.e., the monoclinic $Gd_5Si_2Ge_2$-type, gives a high R value of 0.1602 for 87 parameters and 1394 reflections. Such a high R value is mainly due to the overlap of reflections from both domains.

In an effort to find a specimen showing just a single type, i.e., either Sm_5Ge_4- or $Gd_5Si_2Ge_2$-type, we tested numerous crystals. Crystal **3**, whose reciprocal (*hk*1) slice is shown in Figure 3c, shows only the reflections corresponding to the orthorhombic Sm_5Ge_4-type, unlike the previous two cases. However, all efforts to produce

(16) (a) The twin observed here is a nonmerohedral twin, where only a small fraction of reflections from two twin components can be superimposed, while the majority of the reflections remain unaffected by the twinning. Because of the twin relationship $k' = k - (2/9)h$,[16b] the two twin domains coincide almost exactly when $|h| = 0$ or 9. When $|h| = 4$ or 5, the reflections from the two individuals significantly overlap one another. (b) The twin law obtained here is the same as the one from $Gd_5Si_2Ge_2$. For the twin law found in $Gd_5Si_2Ge_2$, see Meyers, J.; Chumbley, S.; Choe, W.; Miller, G. J. *Phys. Rev.* **2002**, *B66*, 012106/1.

(17) For examples of pseudo-merohedral twins, see (a) Herbst-Irmer, R.; Sheldrick, G. M. *Acta Crystallogr.* **1998**, *B54*, 443−449. (b) Reger, D. L.; Little, C. A.; Young, V. G., Jr.; Pink, M. *Inorg. Chem.* **2001**, *40*, 2870. (c) Colombo, D. G.; Young, V. G., Jr.; Gladfelter, W. L. *Inorg. Chem.* **2000**, *39*, 4621. (d) Schweitzer, J. W.; Martinson, L. S.; Baenziger, N. C.; Swenson, D. C.; Young, V. G., Jr.; Guzei, I. *Phys. Rev.* **2000**, *B62*, 12792. (e) Cooper, R. I.; Gould, R. O.; Parsons, S.; Watkin, D. J. *J. Appl. Crystallogr.* **2002**, *35*, 168.

Table 2. Atomic Positions and Equivalent Thermal Displacement Parameters in the Crystal Structures of Crystal 3 ($Gd_5Si_{1.5}Ge_{2.5}$) at 163 and 292 K[a]

	x	*y*	*z*	occupancy	U_{eq} (Å^2)
			292 K		
Gd1	0.97983(8)	0.40028(4)	0.17893(8)	1	0.0103(2)
Gd2	0.62549(8)	0.38268(4)	0.83703(8)	1	0.0091(2)
Gd3	0.20681(11)	0.75	0.49980(11)	1	0.0092(2)
T1 (T′)	0.7851(2)	0.45674(12)	0.5340(2)	0.666(6)	0.0097(6)
T2 (T′)	0.0804(4)	0.75	0.1098(3)	0.512(8)	0.0090(9)
T3 (T)	0.3199(3)	0.75	0.8675(3)	0.562(8)	0.0101(8)
			163 K		
Gd1	0.02221(12)	0.40335(6)	0.18236(10)	1	0.0072(4)
Gd2	0.67909(11)	0.37729(6)	0.82311(10)	1	0.0065(4)
Gd3	0.14941(16)	0.75	0.50944(14)	1	0.0058(4)
T1 (T′)	0.8462(3)	0.45972(16)	0.5296(3)	0.690(8)	0.0075(9)
T2 (T′)	0.0237(5)	0.75	0.1024(4)	0.526(10)	0.0061(14)
T3 (T)	0.2689(5)	0.75	0.8707(4)	0.523(10)	0.0058(13)

[a] All the T and T′ sites are fully occupied with Si and Ge, but only Ge occupations are listed.

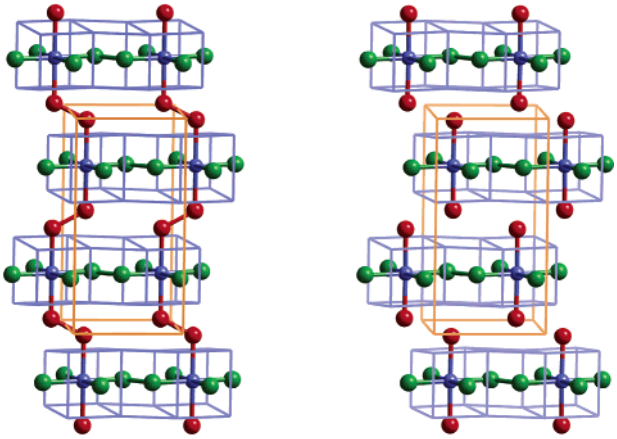

Figure 4. Crystal structure of $Gd_5Si_{1.5}Ge_{2.5}$, determined for crystal **3**. (left) Gd_5Si_4-type in the ferromagnetic state and (right) Sm_5Ge_4-type in the paramagnetic state (room temperature). Gd atoms are in blue; (Si,Ge) atoms inside the slabs are in green; (Si,Ge) atoms between the slabs are in red.

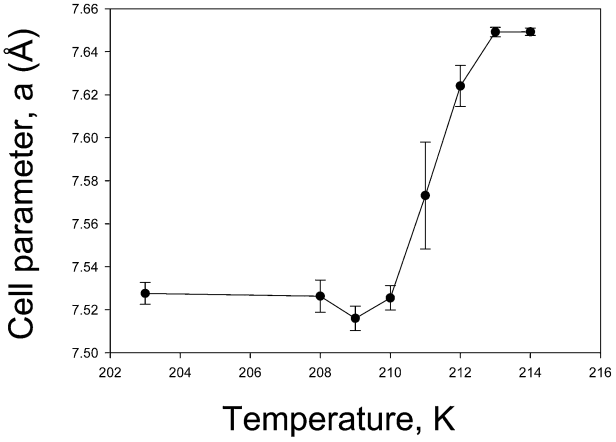

Figure 5. Phase transition in $Gd_5Si_{1.5}Ge_{2.5}$ monitored by the change in cell parameter *a*. The transition temperature is around 211 K.

and find monoclinic $Gd_5Si_2Ge_2$-type crystals with the $Gd_5Si_{1.5}Ge_{2.5}$ composition have failed. When we face a delicate structural problem such as this, X-ray single crystal diffraction has an advantage over X-ray powder diffraction. Although X-ray powder diffraction can distinguish both structure types in the bulk materials, it cannot identify detailed information about the intimate structural relationship between two crystalline phases. Herein, we report the single-crystal data only for crystal **3** because the datasets for crystal **1** and **2** are not of sufficient quality due to overlap of the reflections which originate from the two crystalline domains. The X-ray crystallographic data and atomic coordinates at 292 and 163 K for crystal **3** are listed, respectively, in Tables 1 and 2. The refined compositions of the crystalline specimen are $Gd_5Si_{1.59(4)}Ge_{2.41}$ at 292 K and $Gd_5Si_{1.57(4)}Ge_{2.43}$ at 163 K.

Structure. At 163 K $Gd_5Si_{1.5}Ge_{2.5}$ in specimen **3** crystallizes in space group *Pnma* and belongs to the Gd_5Si_4-type. The structure at 292 K also crystallizes in the same space group, but belongs to the Sm_5Ge_4-type (see Figure 4a and b for both structure types). The two-dimensional $^{\infty}_{2}[Gd_5(Si_xGe_{1-x})_4]$ slabs are the fundamental building unit of both structures. These slabs are built from 3^2434 nets of Gd atoms.[18] Two adjacent Gd 3^2434 nets create the slab, composed of distorted Gd_8 cubes and Gd_6 trigonal prisms. Each Gd_8 cube is filled with another Gd atom, and two face-sharing Gd_6 trigonal prisms accommodate a (Si,Ge)−(Si,Ge) dimer, consequently forming two-dimensional $^{\infty}_{2}[Gd_5(Si_xGe_{1-x})_4]$ slabs. The key difference between the two structure types is how these slabs are connected. At 163 K, all the interslab (Si,Ge) atoms are connected to one another, but at 292 K, all the interslab atoms become isolated. The interslab (Si,Ge)−(Si,Ge) distance changes from ca. 2.6 Å (163 K) to 3.5 Å (292 K).

Phase Transition. The magnetically coupled structural transitions in the $Gd_5(Si_xGe_{1-x})_4$ system for $x \leq 0.503$ can be monitored with changing temperature by using the crystallographic *a* parameter, because the change in *a* lattice parameter during the phase transition is quite drastic, typically five times greater than that along the other two crystallographic directions.[9] Figure 5 illustrates the change in the crystallographic *a* parameter for crystal **3** as the temperature varied from 203 to 214 K, and indicates the transition temperature to be ca. 211 K. Because the Curie temperature T_c shows linear dependence on the Si/Ge ratio in $Gd_5(Si_xGe_{1-x})_4$ ($x \leq 0.503$), it is possible to extrapolate the transition temperature for $Gd_5Si_{1.5}Ge_{2.5}$ from magnetic measurements. The expected T_c for $Gd_5Si_{1.5}Ge_{2.5}$ is 208 K, which is in good agreement with the temperature of the structural transition, 211 K.[11d] Therefore, T_c is an ideal parameter to monitor any compositional changes in the $Gd_5(Si_xGe_{1-x})_4$ series.

(18) The 3^2434 net is a popular net pattern found in intermetallic solids. See Hyde, B. G. Andersson, S. *Inorganic Crystal Structures*; Wiley: New York, 1989; pp 290−291.

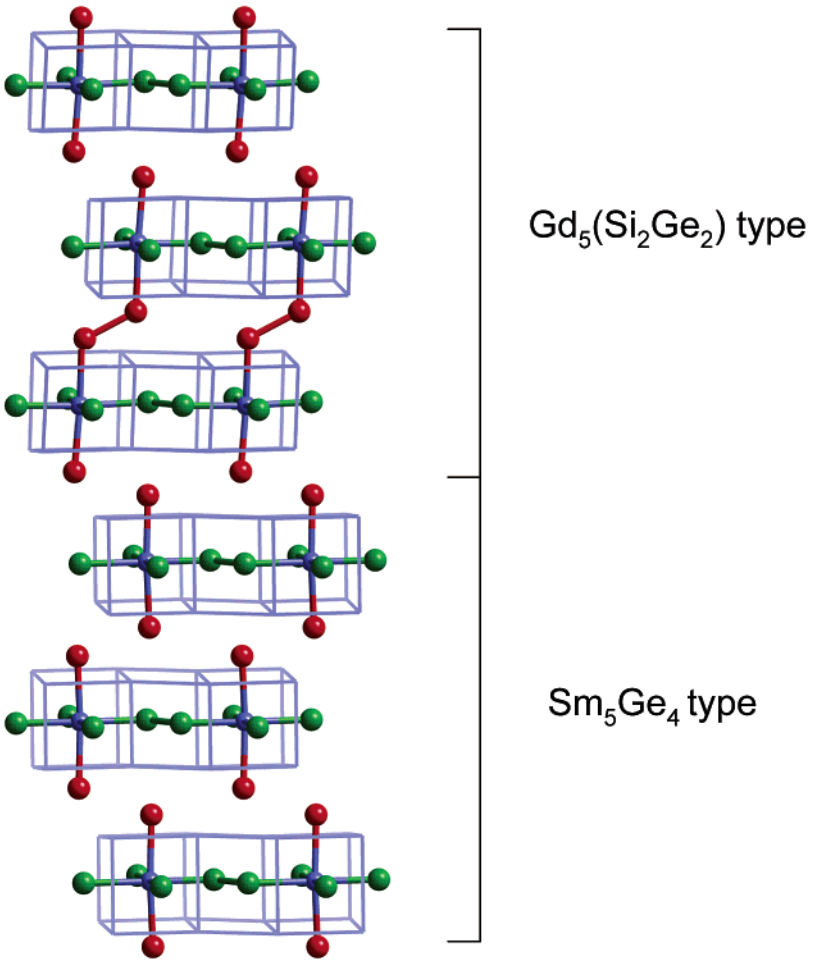

Figure 6. Structural model for the interface between two structure types: Sm_5Ge_4 and $Gd_5Si_2Ge_2$. Depending on the pattern of the dimer formation/cleavage, one can generate Sm_5Ge_4- and $Gd_5Si_2Ge_2$-type structures.

Coexistence of Orthorhombic and Monoclinic Phases. As mentioned in the Structure Refinement section, crystals **1** and **2** contain both monoclinic and orthorhombic phases, whereas the relative portion of each phase can differ from crystal to crystal. The coexistence of multiple crystalline domains in a single crystal is quite exceptional. In other words, these two crystalline domains have, in fact, three components: two twinned monoclinic components and one orthorhombic component. Furthermore, there is a special geometric relationship among the three components. First of all, the two monoclinic components are related by rotation along the monoclinic **a** axis, which becomes the twin axis. Then, the orthorhombic phase shares its **a** axis with the monoclinic twin axis. On the basis of these special orientations of the monoclinic and the orthorhombic reciprocal lattices, we can build a structural model for the interface between the orthorhombic Sm_5Ge_4- and monoclinic $Gd_5Si_2Ge_2$-types. Figure 6 reveals an atomic-level model which matches with the reciprocal lattices shown in Figures 4 and 5. As can be seen, it is possible to stack the Sm_5Ge_4-type structure on top of the $Gd_5Si_2Ge_2$-type or vice versa. This is due to the dimers residing in the slabs. In the "$Gd_5Si_4 \rightarrow Sm_5Ge_4$" type transition, all dimers in the slabs break. In contrast, in the "$Gd_5Si_4 \rightarrow Gd_5Si_2Ge_2$" type transition, the dimers break in every other slab. If one considers the introduction of stacking faults (essentially "mistakes" in such registry), it is possible to create two crystalline domains. Therefore, depending on the "zipping" action (dimer formation) and "unzipping" action (dimer cleavage), the "nanoscale zippers" create regular or irregular patterns of dimer sequences across the crystallographic **b** axis. Previous magnetic measurements on $Gd_5Si_{1.5}Ge_{2.5}$ show the existence of two magnetic heterogeneous domains, which, according to our finding, is due to two distinct crystalline domains. The metallography of the polycrystalline material is shown in Figure 7. TEM examination of $Gd_5Si_{1.5}Ge_{2.5}$ shows no indication of secondary phases. However, the SAD patterns obtained clearly indicate that two different crystalline domains could coexst. In Figure 7, as SAD patterns shows, the orthorhombic phase appears at both ends while the monoclinic phase emerges in the middle. Such findings also support our X-ray single-crystal experiments.

Shear Movements and "Nanoscale Zippers". The $Gd_5(Si_xGe_{1-x})_4$ structures which exhibit bond-breaking and reforming are shown in Figure 8. In this figure, just the dimers and $^{\infty}_{2}[Gd_5(Si_xGe_{1-x})_4]$ slabs are illustrated to highlight the movement of the slabs. In both $Gd_5Si_2Ge_2$ and $Gd_5Si_{1.5}Ge_{2.5}$, the bond-cleavage occurs simultaneously with the shear movement of the slabs,[6] but $Gd_5Si_{1.5}Ge_{2.5}$ undergoes a shear movement pattern different from that ot $Gd_5Si_2Ge_2$. In the Si-richer phase, $Gd_5Si_2Ge_2$, the slabs shift in pairs, whereas in the Si-poorer phase, $Gd_5Si_{1.5}Ge_{2.5}$, alternating slabs shift. There is another related "nanoscale zipper" in the literature, which results from a different type of shear

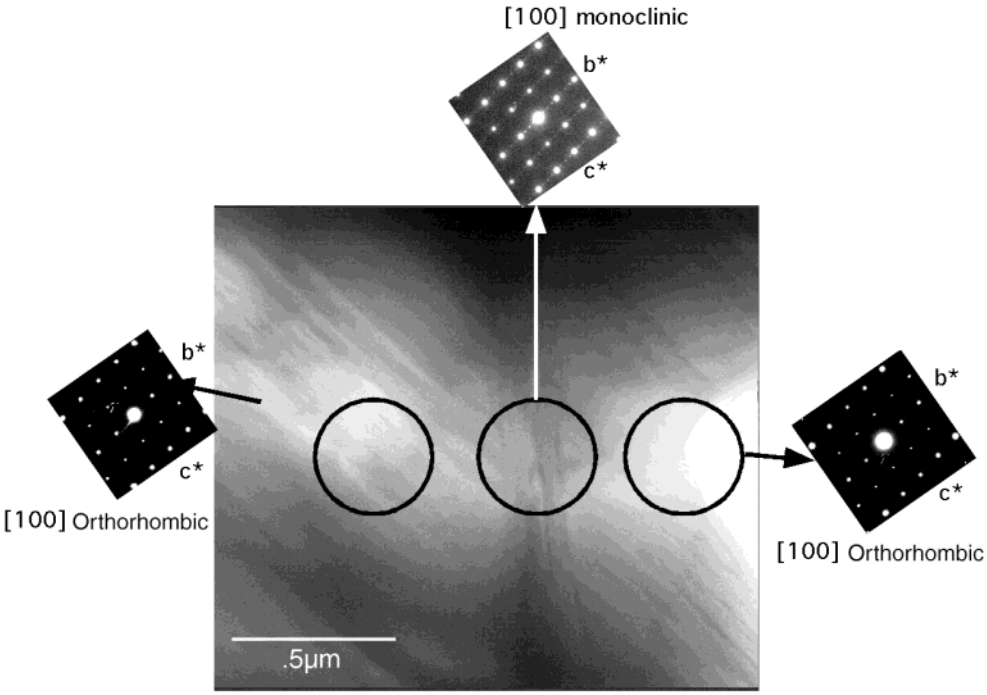

Figure 7. TEM for polycrystalline $Gd_5Si_{1.5}Ge_{2.5}$. Selected area diffraction patterns are shown across the specimen, which show orthorhombic Sm_5Ge_4-type on the left and right sides and monoclinic $Gd_5Si_2Ge_2$ type in the middle.

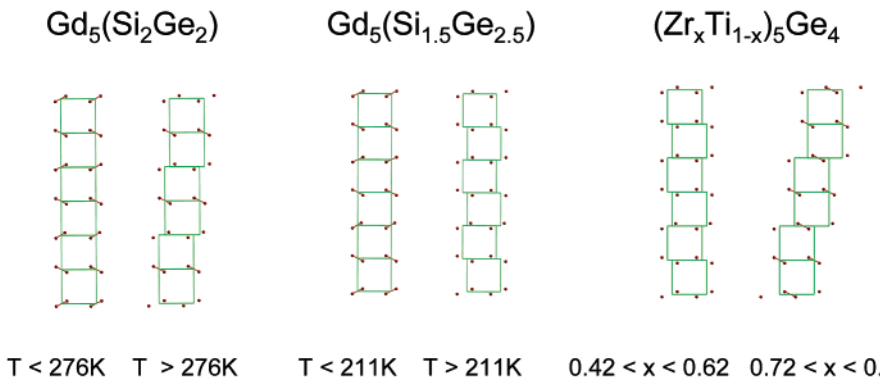

Figure 8. Shear movements found in "nanoscale zippers". Only the slabs and the dimers between the slabs are shown. Shear movements taking place (left) during temperature changes in $Gd_5Si_2Ge_2$, (middle) during temperature changes in $Gd_5Si_{1.5}Ge_{2.5}$, (right) for compositional changes in $(Zr_xTi_{1-x})_5Ge_4$.

movement of this type of slab.[19] $(Zr_xTi_{1-x})_5Ge_4$ shows an interesting transition as x varies from 0.42 to 0.78, where it adopts the orthorhombic Sm_5Ge_4-type with $0.42 < x < 0.62$ and monoclinic $Y_2Mo_3Ge_4$-type with $0.72 < x < 0.78$.[19] In this structure type, the dimers between the slabs do not adopt a herringbone pattern found in the other three structure types shown in Figure 8a and b.

Conclusion. The crystal structure of $Gd_5Si_{1.5}Ge_{2.5}$ structure shows its unique ability to adopt two different structure types in a crystalline sample: the Sm_5Ge_4-type and $Gd_5Si_2Ge_2$-type. The structural variation is due to the "nanoscale zipping" action, which occurs between the $^{\infty}_{2}[Gd_5(Si_xGe_{1-x})_4]$ slabs found in $Gd_5(Si_xGe_{1-x})_4$ system. In $Gd_5Si_{1.5}Ge_{2.5}$, the $^{\infty}_{2}[Gd_5(Si_xGe_{1-x})_4]$ slabs are held together by either "dimers" or isolated Si or Ge atoms. Therefore, depending on the pattern of bond cleavage/formation, different structures can coexist. X-ray data, as well as selected area diffraction experiments, confirm the coexistence of the orthorhombic Sm_5Ge_4-type and monoclinic $Gd_5Si_2Ge_2$-type in the crystalline sample of $Gd_5Si_{1.5}Ge_{2.5}$.

Acknowledgment. The Ames Laboratory is operated by Iowa State University for the U. S. Department of Energy (DOE) under contract W-7405-ENG-82. This work was supported by the Office of Basic Energy Sciences, Materials Science Division of the U. S. DOE. We thank Vitalij Pecharsky and Karl A. Gschneidner, Jr. for many fruitful discussions.

Supporting Information Available: An X-ray crystallographic file, in CIF format, containing information for $Gd_5Si_{1.5}Ge_{2.5}$ (crystal **3**) at 163 and 292 K. This material is available free of charge via the Internet at http://pubs.acs.org.

CM020928L

(19) Richter, K. W.; Franzen, H. F. *J. Solid State Chem.* **2000**, *150*, 347.